

On the Influence of Increased Stator Leakage Inductance in Single Tooth Wound Synchronous Reluctance Motors

C. M. Donaghy-Spargo, *Member IEEE*, B.C. Mecrow, *Member IEEE*, J. D. Widmer

Abstract— This paper explores the leakage inductance of a single tooth wound synchronous reluctance motor and its influence on motor performance. It is shown that the stator leakage inductance heavily influences the true saliency ratio in synchronous reluctance motors and a large stator leakage inductance has a serious detrimental impact on the operating power factor. It is also shown through analytical and FEA analysis that synchronous reluctance motors with single tooth windings suffer an inherent high stator leakage inductance that is dominated the air gap harmonic leakage component, derived from the significant stator MMF harmonics experienced with this winding type. This explains for the first time the experimental results showing a low operating power factor compared to a distributed wound machine. Measurement of the stator leakage inductance is attempted on a prototyped machine and the standardized method is found to be lacking when single tooth windings are employed.

Index Terms— leakage inductance, single tooth windings, synchronous reluctance motors, removed rotor.

I. INTRODUCTION

IT is well known that the stators of synchronous reluctance machines are traditionally wound with polyphase distributed stator coils, identical to that of the induction machine. The synchronous reluctance motor is a popular area of research and is under certain circumstances replacing the induction motor in variable speed drive due to their advantages [1-3]. A logical step forward in advancing synchronous reluctance technology is to examine the possibility of migration from polyphase distributed windings to fractional slot concentrated windings (single tooth coils), as suggested by the authors [4,5], with the aim of improving performance and enjoying the various benefits of these single windings. Many authors have considered synchronous reluctance motor design improvements [6-9], but are all with distributed winding arrangements. A large number of papers are concerned with rotor flux barrier optimization, for example [10,11] or

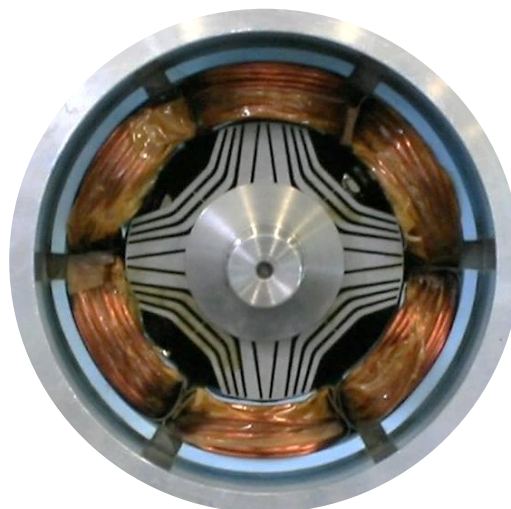


Fig. 1 Single-tooth coil synchronous reluctance motor (6 slot 4 pole).

permanent magnet assisted variants [12,13]. An exploration of the effect of stator leakage inductance cannot be found in the literature and this inductance is usually neglected in literature. The authors have previously proposed the use of single tooth wound synchronous reluctance machines to realize a higher torque density and energy conversion efficiency machine [4], Fig. 1 shows the rotor of the experimentally verified prototype.

The proposed machine was shown to have a higher energy conversion efficiency compared to the traditionally wound machine, however, it was found to suffer from a low power factor and higher torque ripple [5]. The torque ripple has been addressed in [14], however, the issue of low power factor has not been addressed. The low operating power factors reduces the effective inverter utilization and increases the attached converter current – the motor power factor as measured experimentally was 0.48-0.5. This is very low, compared to an equivalent induction machine of approximately and conventional synchronous reluctance motor, estimated at 0.85 and 0.7 respectively [5]. This reduced power factor is a major obstacle to industrial adoption and it must be further understood.

The present paper fills the gap in the literature and technical knowledge, it explores the stator leakage inductance of synchronous reluctance motors with single tooth windings and its effect on motor performance. The 6 slot 4 pole prototype is used throughout, where the effect of increased stator leakage

Manuscript received May 21, 2017; revised Month August, 2017; accepted October 19, 2017.

C. M. Donaghy-Spargo is with the Department of Engineering, University of Durham, Durham, DH1 3LE, UK, (e-mail: christopher.spargo@dur.ac.uk). B.C. Mecrow and J. D. Widmer are with the School of Engineering, Newcastle University, Newcastle upon Tyne, NE1 7RU, UK.

inductance on the saliency ratio and power factor is explored, the inductance components calculated and the dominant leakage identified, arriving at an explanation of the observed low power factor. Comparison, where appropriate, is made with conventionally wound synchronous reluctance motors. An attempt at measuring the stator leakage inductance via the removed rotor test is also reported in this paper.

II. SYNRM INDUCTANCES & SALIENCY RATIO

The following two sections explore the functional relationships of the synchronous reluctance motors power factor and numerical examples are used where appropriate. When modelling the synchronous reluctance motor, the orthogonal axis inductances are typically the key parameters used for performance calculation and estimation. These orthogonal axis inductances can be expressed as follows [15];

$$L_d(i_d) = L_{md}(i_d) + L_{s\sigma} \quad (1)$$

$$L_q(i_q) = L_{mq}(i_q) + L_{s\sigma} \quad (2)$$

Where L_{md} and L_{mq} are the d - and q -axis magnetizing components respectively as functions of their axis currents i_d & i_q and $L_{s\sigma}$ is the stator leakage inductance. It is well known that ‘saliency ratio’ is the key figure of merit of the synchronous reluctance motor [15] as the overall performance of the machine improves with increasing saliency ratio [16]. There are two ‘versions’ of the saliency ratio, the ‘true’ saliency ratio and the ‘magnetizing’ saliency ratio, the former is written;

$$\xi_{\text{true}}(i_d, i_q) = \frac{L_d(i_d)}{L_q(i_q)} = \frac{L_{md}(i_d) + L_{s\sigma}}{L_{mq}(i_q) + L_{s\sigma}} \quad (3)$$

$\xi_{\text{true}} = f(L_{s\sigma})$ The magnetizing saliency ratio neglects the stator leakage inductance term, it is simply the ratio of the d to q -axis magnetizing inductances;

$$\xi_{\text{mag}} = \frac{L_{md}(i_d)}{L_{mq}(i_q)} \quad (4)$$

$\xi_{\text{mag}} \neq f(L_{s\sigma})$ As mentioned, this saliency ratio is required to be high for high torque density, efficiency and power factor [15,16] and $L_{s\sigma}$ has a direct impact. The true saliency ratio should be used in performance calculations. It is clear that the $L_q(i_q)$ inductance in the denominator of the true saliency ratio expression can have a profound impact on that saliency ratio and therefore motor performance. The leakage inductance is clearly seen to be an important parameter;

$$L'_q(i_q) = \lim_{L_{mq} \rightarrow 0} [L_q(i_q)] = L_{s\sigma} \quad (5)$$

Therefore, the stator leakage inductance represents the ‘floor’ of the q -axis inductance, it is the minimum limiting value of a design parameter the motor engineer seeks to minimize as much as possible in any design, in order to maximize motor

performance (torque production, energy conversion efficiency and power factor). A high true saliency ratio is required, in order for the synchronous reluctance motor to compete with the induction motor in industrial variable speed drive applications. Four pole machines are almost universally found in the literature (see Appendix).

III. INFLUENCE OF STATOR LEAKAGE INDUCTANCE

From (3), it is clear that the stator leakage inductance has an effect on the true saliency ratio and its effect is more pronounced with respect to the q -axis inductance as the d -axis magnetizing component. Usually the *direct* axis magnetizing inductance is significantly larger than the *quadrature* axis magnetizing component, by careful design of the rotor flux barrier arrangement [1,10,16]. It can be shown by considering the phasor diagram that the maximum achievable power factor in a synchronous reluctance machine is a function of the saliency ratio and can be determined by [24];

$$\cos(\varphi) = (\xi_{\text{true}} - 1) \frac{\cos(\gamma)}{\sqrt{\xi_{\text{true}}^2 \cot^2(\gamma) + 1}} \quad (6)$$

$$\cos(\varphi)|_{\text{max}} = \frac{\xi_{\text{true}} - 1}{1 + \xi_{\text{true}}} \quad (7)$$

$$= \frac{L_{md} - L_{mq}}{L_{md} + L_{mq} + 2L_{s\sigma}} \quad (8)$$

Here φ is the voltage-current phase angle and γ the stator current angle. Therefore, from (7) if the true saliency ratio is reduced from the ideal value of *magnetizing* saliency ratio ξ_{mag} by the influence of the stator leakage inductance $L_{s\sigma}$ to a reduced value of *true* saliency ratio ξ_{true} , the power factor will increasingly suffer with lowering ξ_{true} , noting the $2L_{s\sigma}$ dependence on the denominator of (8). Here $\cos(\varphi)|_{\text{max}}$ decreases as a direct result of a reduced true saliency ratio. Therefore, the saliency ratio has an increased sensitivity to the q -axis inductance, and therefore, the stator leakage inductance plays a key role in determining the true saliency and consequently the performance of the machine - the stator leakage inductance should not be general ignored. To illustrate the influence of the true saliency ratio on the power factor of the synchronous reluctance motor, Figure 2 shows a family of power factor curves as a function of current angle for various true saliency ratios. A true saliency ratio $\xi_{\text{true}} = 50$ is unrealistic in any practical design, it is however included for comparison. A good design of conventional synchronous reluctance motor may be able to achieve a true saliency ratio $\xi_{\text{true}} = 10$, of which a maximum power factor of 0.81 can be achieved at a current angle $70 \leq \gamma \leq 75$ degrees. A poorer rotor design, with a true saliency ratio $\xi_{\text{true}} = 5$, can only achieve a maximum power factor of 0.66 at a current angle of $65 \leq \gamma \leq 70$ degrees and a primitive rotor design, perhaps a salient pole generator rotor with the rotor DC windings removed, achieving a true saliency ratio $\xi_{\text{true}} = 2$ can only achieve a maximum power factor of 0.33 at a current angle of $50 \leq \gamma \leq 55$ degrees. It is seen that while the maximum power factor reduces with reducing true saliency ratio, the

current angle at which this *maximum power factor* is achieved also changes. This ‘maximum power factor’ is achieved when the motor is operated such that the voltage headroom is maximized and for minimum apparent power requirement at a given torque-speed set point. In order to compete with the induction motor, the synchronous reluctance motor is operated under maximum torque per ampere control for maximum torque density and energy conversion efficiency (neglecting iron loss), as such, the operating power factor is generally less than the theoretical maximum [15]. The real power P developed by a synchronous reluctance motor can be expressed as [17];

$$P \propto (L_d - L_q) \sin(2\gamma) \quad (9)$$

Therefore, for maximum torque per ampere operation, $\sin(2\gamma) \rightarrow 1 \Rightarrow \gamma = 45$ degrees, and consequently a lower power factor, but higher energy conversion efficiency is typically achieved under these circumstances. From (9), it is usually assumed that the stator leakage inductance has no direct effect on the torque producing capability as $L_d - L_q = (L_{md} + L_{s\sigma}) - (L_{mq} + L_{s\sigma}) = L_{md} - L_{mq}$.

Now, considering a synchronous reluctance motor with a high magnetizing saliency ratio $\xi_{\text{mag}} = 16$, where it is assumed that $L_{md} = 50\text{mH}$ and $L_{mq} = 3\text{mH}$, Figure 3 shows the reduction in true saliency ratio for an increasing stator leakage inductance component between 0 ($\xi_{\text{true}} = \xi_{\text{mag}}$) and 0.35.p.u. ($\xi_{\text{true}} = 3.3$). The results show a consistent reduction in the maximum power factor capability of the machine and the stator current angle at which it occurs.

When $L_{mq} < L_{s\sigma}$ the stator leakage inductance is dominant in the denominator and in the example, this occurs when $L_{s\sigma} > 0.06$ p.u., thus for $L_{s\sigma} = 0.1$ p.u., the magnetizing saliency ratio is reduced to $\xi_{\text{true}} = 6.9$ with a reduction in maximum power factor from 0.85 to 0.75, with further increases in stator leakage reducing the power factor further. At a leakage inductance of 0.35 p.u. the motor power factor capability is reduced to 0.54. Figure 4 clearly shows the corresponding decrease in motor power factor with increasing stator leakage inductance. It is clear from the results in Fig. 3 & 4 that increased stator leakage inductance is detrimental to machine power factor and can significantly reduce the desirability of such machines when considering replacement of induction machines in industrial applications. That the magnetizing saliency of $\xi_{\text{mag}} = 16$ is representative of a ‘good’ design.

To achieve a saliency ratio of this magnitude, a transversely laminated rotor could be used, but may more easily be achieved by using an axially laminated rotor – here the laminations are arranged axially along the length of the motor, rather than transverse, which are typically formed into the correct rotor shape [15] In the axially laminated design, air-gaps between numerous laminations in the q -axis minimize the q -axis flux whilst the magnetic flux in the d -axis is maximized, leading to larger saliency.

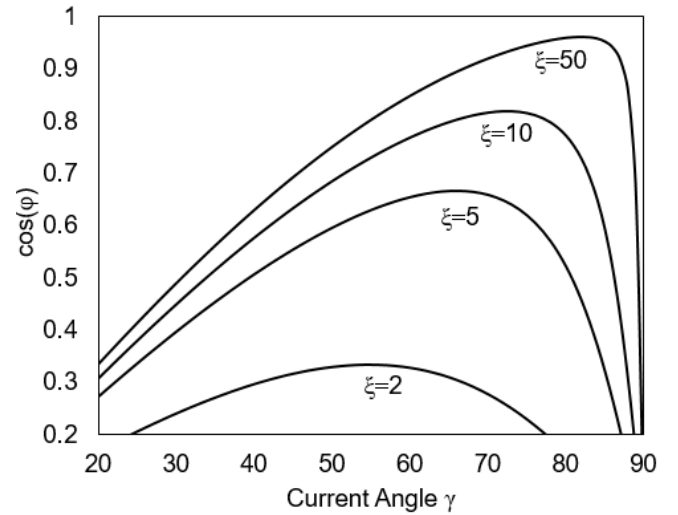


Fig. 2 Power factor - function of current angle, various saliency ratios.

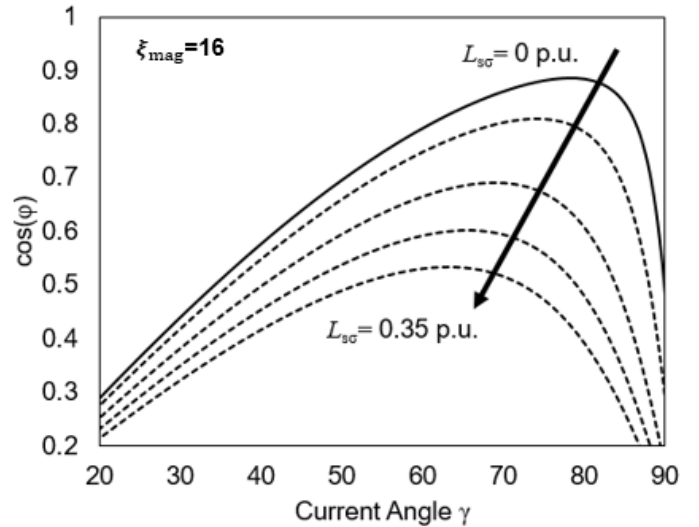


Fig. 3 Power factor curves as a function of current angle for $\xi_{\text{mag}} = 16$ and increasing stator leakage inductance.

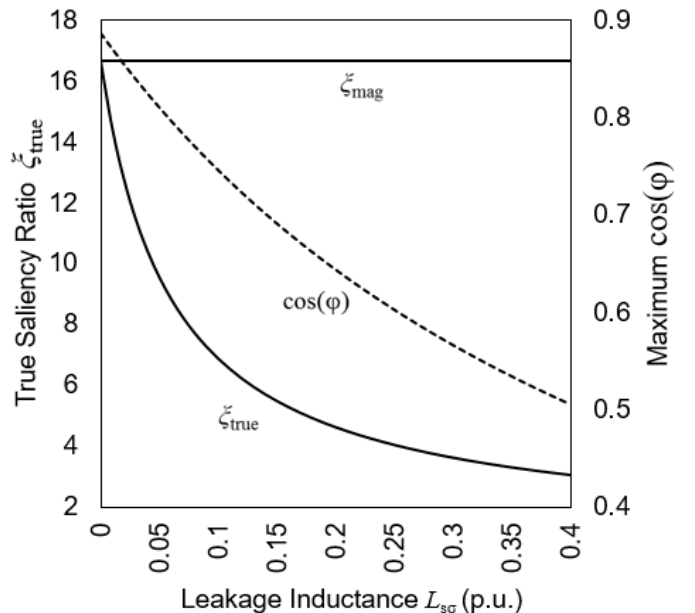


Fig. 4 True saliency ratio ξ_{true} and maximum power factor capability as a function of per-unit stator leakage inductance with $\xi_{\text{mag}} = 16$.

IV. SINGLE TOOTH WOUND SYNRM CONCEPT

The authors have previously suggested the use of single tooth windings to improve the energy conversion efficiency of the synchronous reluctance motor [4,5,14], the ‘cSynRM’. A motor was designed, constructed and experimentally verified that utilized a double layer fractional slot concentrated winding arrangement, with coils that span a single tooth. The motor exhibited a high energy conversion efficiency (>91% at 3.5kW rated power) due to the high slot fill factors achieved with the single tooth wound coils (slot fill factor, $S_{FF} = 60\%$), but a higher torque ripple (~40%) and lower power factor (0.5), compared to a conventionally wound synchronous reluctance motor. The torque ripple was analyzed in [14] and found to be due to a 2nd order counter-rotating 8 pole field interacting with the rotor harmonic saliency, causing significant torque oscillation. The motor has of 6 slots, constructed from a segmented stator core arrangement where the coils are pre-wound onto each segment before assembly [18]. The transversely laminated rotor consists of 4 rotor poles with optimized flux barrier design. Figure 1 shows the radial cross section of the prototyped machine, the stator of which stator has a single tooth winding with a number of *slots per pole per phase* of $q = 0.5$, where the rotor pole pitch is only 1.5x the stator tooth pitch, leading to asymmetry of the stator MMF function. The harmonic winding factors k_{wv} of order v are constant across all harmonics with the winding factor $k_{wv} = 0.866 \forall v$, leading to significant space harmonic content in the stator MMF wave and therefore in the airgap flux density wave [15]. Due to the choice of slot-pole combination both *odd* and *even* harmonics can exist in the stator MMF spectrum where usually the even harmonics are eliminated by the symmetry of a sinusoidally distributed integer or fractional slot winding. Figure 5 shows the winding factors and 3 phase MMF spectrum for this winding configuration, which clearly includes both odd and even harmonics. Compared to a distributed winding machine, the stator MMF of which does not contain such rich harmonic content, the airgap harmonic content in the cSynRM is significant. Usually in the distributed winding machine the MMF harmonics are a minimum due to the distribution of the coils and also the pitching of the coils to fine-tune the harmonic winding factors, whilst maximising the fundamental winding factor. It must also be noted that the fundamental winding factor of the 6 slot 4 pole double layer concentrated winding is low, $k_{w1} = 0.866$, when compared to a distributed winding machine that would typically have a $k_{w1} > 0.9$.

Therefore the single-tooth wound machine is immediately at a disadvantage, compounded by increased harmonic content. However, this machine is competitive for some applications, despite the poor winding factors and increased harmonics. Due to the parasitic effects, the rotor lamination profile must be carefully designed - there are clear consequences of adopting such windings for the synchronous reluctance motors in addition to the benefits described elsewhere [19]. The emphasis in this paper is on the impact with regard the stator leakage inductance, particularly the harmonic contribution and the effect upon motor power factor.

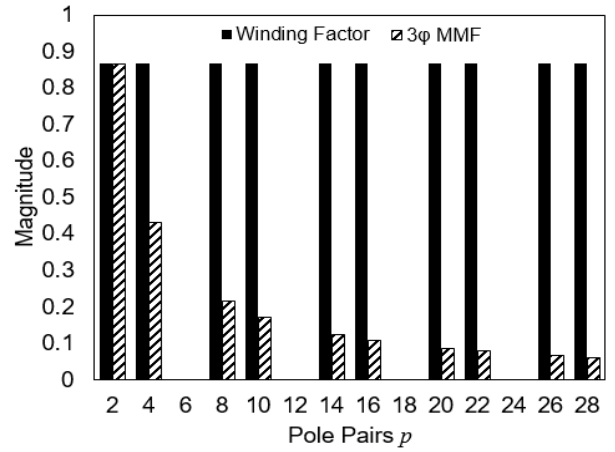


Fig. 5. Winding factors of the 6-slot 4-cSynRM

V. PROTOTYPED MOTOR

The 6 slot 4 pole motor was prototyped, the laminations being cut from M250-35A material using electro-discharge machining techniques. The machine was first described and analysed in [14], with further analysis in [4] and experimental validation in [5,18] the proposed motors performance was experimentally verified both statically (magnetic circuit characterisation) and dynamically on a dynamometer test rig. Figure 6 shows the prototyped rotor in detail. Removed rotor testing is reported in Section VIII of this paper.

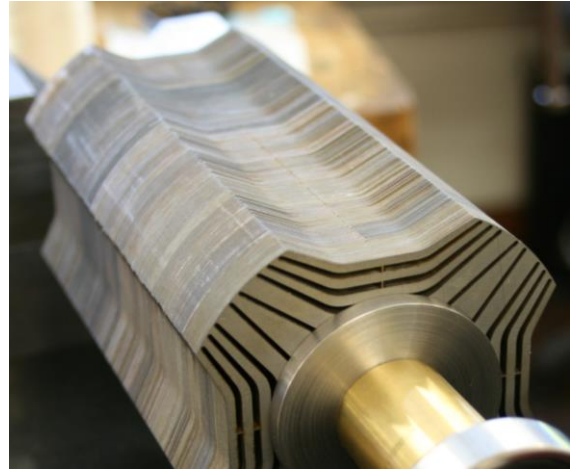


Fig. 6. The prototype rotor showing lamination profile.

VI. GEOMETRIC LEAKAGE INDUCTANCE

The inductances are very important for machine performance - the orthogonal axis inductances of the synchronous reluctance machine are best calculated through FEA due to the saturation in the rotor webbing and stator tooth tips, however analytical approximation is common for the stator leakage inductance, comprising a number of components, for an m -phase machine of stack length L , number of stator slots Q and turns N ;

$$L_{s\sigma} = \mu_0 \left(\frac{4mN^2L}{Q} \right) \left(\lambda_s + \frac{l}{L} \lambda_e + \lambda_{tt} + \lambda_h \right) \quad (10)$$

Where λ_s , λ_e , λ_{tt} and λ_h are the slot leakage, end winding, tooth tip and air-gap harmonic permeance coefficients

respectively. The permeance coefficients and associated inductances are calculated in this paper following the methods described by Gieras [20]. Two distinct contributions to the leakage inductance can be identified;

1. Non-airgap crossing: *geometric* leakage ($\lambda_s, \lambda_e, \lambda_{tt}$)
2. Airgap crossing: *harmonic* leakage (λ_h only)

Based on the machine geometry and winding, the geometrical permeance coefficients $\lambda_s + \frac{l}{L}\lambda_e + \lambda_{tt}$ can be estimated for the 6 slot 4 pole design. The procedure follows that in standard text book approach given by Pyhronen [17] and Gieras [20], as well being employed in [21] for PM machines – the full equations are not repeated here and the reader is referred to the references. The purpose of the present and following sections is to identify the dominant stator leakage component in the design, firstly the construction leakage inductance is examined and then the increased MMF harmonic contribution to the stator leakage inductance. In the following expressions, $G = \mu_0 \left(\frac{4mN^2L}{Q} \right)$, which is defined as the inductance coefficient.

A. Lumped End Winding Leakage Inductance

The end winding leakage inductance due to flux leakage in the end region around the end turns of the stator coils, which is governed by the end winding geometry. The lumped end winding leakage inductance L_{ew} can be approximated by;

$$L_{ew} = \frac{G\lambda_{ew}}{L} = \frac{G}{L} \cdot f(w_c, l_e) \quad (11)$$

Where w_c is related to the coil span and l_e the length of the end turns. The analytically calculated lumped end winding inductance is 138.15 μ H, this is agreeable with the inductance calculation using the software which uses a finite element based method with a 3D end winding model to calculate this leakage component and suggests an end winding leakage inductance of $L_{ew}=139.5\mu$ H which has small difference from the analytical calculation. The end winding leakage inductance is very small due to the tightly wound coils in close proximity to the stator core, reducing the flux leakage in the end winding region.

B. Slot Leakage Inductance

Under normal operation, the slot MMF mostly crosses the air gap and links the rotor, however some of it crosses the slot from tooth to tooth. The slot leakage inductance for the slot geometry in the prototype machine is given as;

$$L_s = G\lambda_s = G \cdot f(\text{slot dimensions}) \quad (12)$$

Where the slot permeance coefficient is a function of the specific geometry of the slot. The calculation assumes that the flux crossed the slot straight and horizontal and does not include the leakage close to the air gap where this assumption becomes invalid, this effect can be modelled as the tooth tip leakage inductance separately. Based on prototypes

dimensions, the slot leakage inductance is found to be $L_s = 1.67$ mH.

C. Tooth Tip Leakage Inductance

The final component of the stator geometric leakage inductance, the *tooth tip leakage inductance*, accounts for slot leakage close to the air gap region;

$$L_{tt} = G\lambda_{tt} = G \cdot f(\text{slot opening dimensions}) \quad (13)$$

Calculation of the tooth tip leakage inductance for the prototype machine dimensions gives $L_{tt} = 181.69\mu$ H.

D. Total Geometric Leakage Inductance

The total geometric leakage inductance is equal to the sum of the components, $L_{s\sigma}^c = 1.99$ mH, the end winding leakage inductance is confirmed through 3D FEA studies at 0.138mH. The dominant geometric component is the slot leakage inductance.

VII. HARMONIC LEAKAGE INDUCTANCE

To the present point in this paper, only non-air gap crossing components of the stator leakage inductance have been considered. The air gap harmonic leakage inductance is the only leakage to cross the air gap boundary. This leakage, also known as the ‘differential leakage inductance’ is caused by space stator MMF space harmonics that create harmonic fluxes that cross the air gap and link the rotor, this is leakage as it is asynchronous to the rotor synchronous speed and does not facilitate mean torque production. The harmonic leakage, based on the air gap space harmonic content, can be determined using a harmonic permeance coefficient model;

$$L_h = G \cdot \lambda_h \quad (14)$$

and the harmonic leakage factor λ_h is defined as;

$$\lambda_h = \sum_{v=2}^{\infty} \left(\frac{k_{w1}}{vk_{wv}} \right)^2 \quad (15)$$

This is a figure of merit relating to the harmonic content of the air gap MMF wave. Only harmonics created by the winding occur in the summation and it excludes the fundamental torque producing (magnetizing) component. The air gap harmonic leakage factor for common slot-pole combinations with viable windings is presented in Table. I. In the case of the single tooth wound synchronous reluctance motor under study, it is clear that with $q = 0.5$, the stator MMF wave contains rich harmonic content (Figure 5), including even harmonics. For a 6 slot, 4 pole motor, the air gap harmonic leakage factor is $\lambda_h = 0.462$. For some slot-pole combinations, $\lambda_h > 1$, here it must be the case that the harmonic leakage dominates over the magnetizing inductance of the machine [22]. For the design and prototyped motor, the air-gap harmonic leakage inductance is evaluated as $L_h = 7.04$ mH. This air gap leakage component is therefore the dominant leakage inductance, being approximately $3.5 \times L_{s\sigma}^c$, the constructional stator leakage inductance. Its dominance will therefore have

profound effect on the power factor and performance of the single tooth wound synchronous reluctance motor. In a conventionally wound machine with integer slot distributed windings, the air gap harmonic leakage factor is of the magnitude of <0.08 [17,20] when $q \geq 2$, compared to the chosen fractional slot concentrated winding of 0.462, which is in agreement with [21,22]. This is a cause for concern, but does provide an explanation to why the power factor is inherently low in the cSynRM motor topology and also illustrates why the stator leakage inductance should be considered a design parameter for the single tooth wound synchronous reluctance motor.

TABLE I
Harmonic Leakage Factors

Poles \ Slots	2	4	6	8	10
3	0.462	4.85		22.4	35.5
6		0.462		4.85	40.1
9			0.462	2.15	3.29
12				0.462	1.95
15					0.462

In relation to the design of a single tooth wound variant of the synchronous reluctance motor, consideration of the slot-pole combination in the machine design is important as the power factor and general machine performance is degraded by high harmonic leakage. From the analytical approximations, it is clear that the dominant leakage component in the 6 slot 4 pole prototype is the air gap harmonic leakage L_h due to the high levels of space harmonic content in the small air gap. A backwards rotating 8 pole MMF has a large contribution (see Figure 5). This acts to degrade the *true* saliency ratio of the machine. Through FEA studies, the motor power factor at rated operating condition calculated and measured experimentally as 0.48-0.5 at the rated operating point, which is very low compared to other machine topologies. The slot and the tooth tip are the second largest components, the end winding leakage component has the lowest contribution. The analysis appears to show that the end effects are low with regard to flux leakage and the major leakage is actually air gap crossing. The sum of the calculated leakage inductances giving a calculated total leakage inductance is $L_{s\sigma}=9.03\text{mH}$. The experimentally verified quadrature axis inductance is approximately $L_q=10\text{mH}$ [4], which fits reasonably well with the calculated results. The magnetizing component in the q -axis position is low due to the multiple flux barrier design and rotor surface cut-out. The stator leakage inductance is dominant here and the harmonic leakage inductance is dominant within the stator leakage inductance. These figures measured axis inductances translates to a motor true saliency ratio of $\xi_{\text{true}} \approx 4$, unsaturated reducing to $\xi_{\text{true}} \approx 2.7$ at the rated operating point, which fits with the measured power factor of 0.46 presented in [14], when Eq. (7) is employed. The power factor is low, however, it is worth noting that if the air gap harmonic leakage was of the magnitude compared to that of a distributed wound machine, the true unsaturated saliency ratio would be closer to 9, rather than 4, leading to a

much higher power factor and improved energy conversion efficiency. At the rated operating point, $\xi_{\text{true}} \approx 2.7$ could rise as high as $\xi_{\text{true}} \approx 8$ and thus by Eq. 7, the power factor would improve to a value of 0.77. This higher power factor is commensurate with that of a conventionally wound synchronous reluctance motor with low leakage inductance. Methods to reduce this harmonic leakage are sought and are the subject of future work. Here, the stator leakage inductance has been considered constant, which is a common assumption. In reality, this leakage inductance will change with saturation & other operating considerations and will be influenced by the difference in the effective air gap between the d - and q -axes. Further work should be undertaken to determine the influence, however, the analysis remains valid that the stator leakage inductance, in the case of the single tooth wound variant is dominated by air gap harmonic leakage. Figure 7 shows the 2D FEA derived and measured d - q axis inductances of the prototype motor. It is seen from the figure that the q -axis inductance is approximately 10mH, the stator leakage inductance is approximately 9mH, illustrating that as it is likely that the rotor has a low q -axis magnetizing inductance by design, the overall q -axis inductance is dominated by this stator leakage inductance as the analysis suggests.

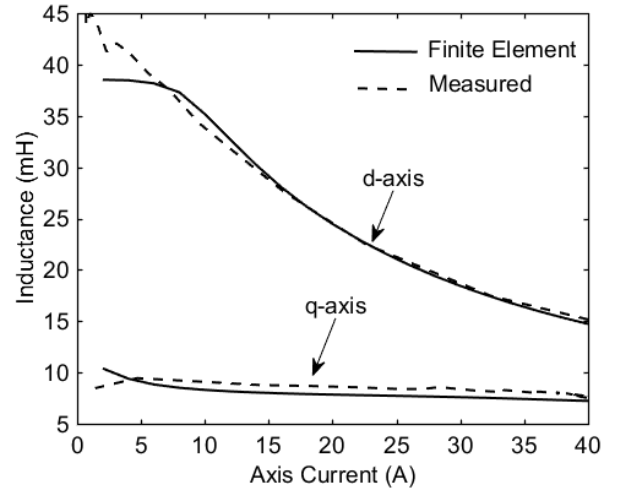


Fig. 7. FEA and measured direct- & quadrature-axis inductances [4]

VIII. REMOVED ROTOR TEST

Measurement of the stator leakage inductance has been neglected in the literature, the standard method of measuring stator leakage inductance in is according to IEEE 115-2009 [23], the so called '*Removed Rotor Test*'. This test involves removing the rotor from the stator and performing a three-phase AC test at rated frequency f and current $I = 21\text{A}$ and an impedance Z measured. A simple search coil of few turns is placed in the air gap to account for any stray air gap fields – this must be negated in the ensuing calculations in order to obtain the constructional stator leakage inductance using conventional circuit theory techniques – a full account can be found in the relevant standard. Two components of the measured reactance X_a are included. The first component of reactance included in the measurement is the stator leakage reactance $X_{s\sigma}$, which includes flux not crossing the air gap

boundary and the stray reactance crossing the air gap boundary X_b . The stator leakage reactance is calculated by $X_{s\sigma} = X_a - X_b$ where X_a is the measured leakage reactance from the applied stator voltage and current with the rotor removed.

The reactance due to the flux crossing air gap boundary created by the stator winding, which is in the space usually occupied by the rotor is typically measured by introducing a search coil of low turns into the void, X_b is then from the search coil voltage and current. The search coil is placed in the rotor void at a diameter slightly less than bore diameter to ensure no inter-slot leakages are included. The coil length is equal to the full stack length and the width of the coil is equal to one rotor pole pitch. The search coil ends must be stretched and positioned away from the end regions as not to link any end winding leakage fluxes that are already included in X_a . Figure 8 shows the prototype machine, rotor removed with the search coil in the void. The stator leakage inductance is calculated with the standard formula;

$$L_{s\sigma} = \frac{X_{s\sigma}}{2\pi f} \quad (16)$$

Here f is the frequency of the injected currents. The removed rotor test is performed on the prototype machine with the rotor removed and an insulated search coil of turns =10 turns placed inside the void. During testing, the machines terminals are connected to a variable three phase sinusoidal supply and currents allowed to flow at the magnitude of the rated current. The terminal and search coil voltages are measured using differential voltage probes and the stator current with a high precision current clamp. The machine terminal voltages is set at $U = 31.3V$, allowing the line current of $I = 21.5A$ to flow, the induced voltage in the search coil is measured as $U_c = 0.81V$. The test is performed for a short duration to prevent any significant temperature rise in the coils. The stator leakage reactance and inductance are calculated using the measured results and are found to be $X_{s\sigma} = 1.041\Omega$ and $L_{s\sigma} = 3.316$ mH respectively.

The results for this component of stator leakage (non-air gap crossing) are higher to that calculated analytically and numerically via the finite element studies. However, the direct measurement of the d -, q -axis inductances using the instantaneous flux linkage technique confirms the analytical results for the overall q -axis inductance (Fig. 7). It must be noted that the presence of the rotor will strongly influence the harmonic leakage. It appears that the standardized test method of the removed rotor test cannot account for, or the rotor search coil remove entirely, the air gap harmonic leakage component leading to inaccurate predictions of the stator leakage geometric inductance, if the air gap crossing component dominates the leakage inductance. In the standard methods, it is assumed that the stator harmonic leakage is low, due to the widespread use of distributed windings with $q > 2$ in both synchronous and asynchronous machines for which this test was originally devised – the search coil is supposed to remove any stray, to allow accurate prediction of the stator

leakage inductance, particularly in large machines as the leakage inductance increases with outer diameter. These machines do not have the same issue of high harmonic leakage as the proposed cSynRM, and as such, the removed rotor test must be used with care when the motor under test is equipped with single tooth windings that have a large air gap harmonic leakage factor. Appropriate techniques are required to be developed and the standards adjusted accordingly for machines with windings that produce a high harmonic leakage component.

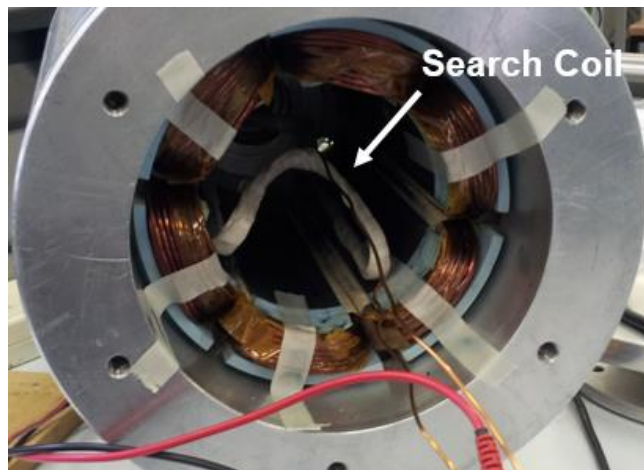


Fig. 8. Removed rotor testing of the prototype machine.

IX. CONCLUSION

The authors have proposed the use of fractional slot concentrated windings (single tooth) winding as a logical step forward in developing the next generation of synchronous reluctance motors to realize higher torque density and efficiency machines for special applications and industrial drives. This paper has explored the stator leakage inductance calculations and measurements as well as its effects on designing a synchronous reluctance motor with this winding type. The stator MMF wave is known to be rich in harmonics and the leakage inductance deserves consideration. The machine inductances are calculated analytically and the air gap harmonic leakage was found to be the dominant leakage component, significantly reducing the true saliency ratio and therefore the machine power factor as demonstrated through FEA and the experimental results. The d - q axis inductance calculations are verified through experimental testing of a 6 slot 4 pole prototype machine and an attempt is made using the standardized techniques to measure the stator leakage inductance. It was apparent that the traditional removed rotor test is inadequate when determining the stator leakage inductance of machines with large air gap harmonic leakage factors. Appropriate choice of slot pole combination must be observed in order to minimise the stator leakage inductance, particularly the air gap harmonic leakage. This issue regarding increased stator leakage inductance is limited to the single tooth wound variant of synchronous reluctance motor; it is suggested that this low power factor is a fundamental limitation of this motor topology.

REFERENCES

- [1] R. R. Moghaddam, F. Magnussen and C. Sadarangani, "Theoretical and Experimental Reevaluation of Synchronous Reluctance Machine," in *IEEE Transactions on Industrial Electronics*, vol. 57, no. 1, pp. 6-13, Jan. 2010
- [2] R. R. Moghaddam and F. Gyllensten, "Novel High-Performance SynRM Design Method: An Easy Approach for A Complicated Rotor Topology," in *IEEE Transactions on Industrial Electronics*, vol. 61, no. 9, pp. 5058-5065, Sept. 2014.
- [3] G. A. Capolino and A. Cavagnino, "New Trends in Electrical Machines Technology—Part II," in *IEEE Transactions on Industrial Electronics*, vol. 61, no. 9, pp. 4931-4936, Sept. 2014
- [4] C. M. Spargo, B. C. Mecrow, J. D. Widmer, C. Morton and N. J. Baker, "Design and Validation of a Synchronous Reluctance Motor With Single Tooth Windings," in *IEEE Transactions on Energy Conversion*, vol. 30, no. 2, pp. 795-805, June 2015
- [5] C. M. Spargo, B. C. Mecrow, J. D. Widmer and C. Morton, "Application of Fractional-Slot Concentrated Windings to Synchronous Reluctance Motors," in *IEEE Transactions on Industry Applications*, vol. 51, no. 2, pp. 1446-1455, March-April 2015
- [6] Z. Gmyrek and M. Lefik, "Influence of Geometry and Assembly Processes on the Building Factor of the Stator Core of the Synchronous Reluctance Motor," in *IEEE Transactions on Industrial Electronics*, vol. 64, no. 3, pp. 2443-2450, March 2017
- [7] J. Ikäheimo, J. Kolehmainen, T. Känäsäkangas, V. Kivelä and R. R. Moghaddam, "Synchronous High-Speed Reluctance Machine With Novel Rotor Construction," in *IEEE Transactions on Industrial Electronics*, vol. 61, no. 6, pp. 2969-2975, June 2014
- [8] M. N. Ibrahim, P. Sergeant and E. E. M. Rashad, "Combined Star-Delta Windings to Improve Synchronous Reluctance Motor Performance," in *IEEE Transactions on Energy Conversion*, vol. 31, no. 4, pp. 1479-1487, Dec. 2016
- [9] S. Taghavi and P. Pillay, "A Novel Grain-Oriented Lamination Rotor Core Assembly for a Synchronous Reluctance Traction Motor With a Reduced Torque Ripple Algorithm," in *IEEE Transactions on Industry Applications*, vol. 52, no. 5, pp. 3729-3738, Sept.-Oct. 2016
- [10] M. H. Mohammadi, T. Rahman, R. Silva, M. Li and D. A. Lowther, "A Computationally Efficient Algorithm for Rotor Design Optimization of Synchronous Reluctance Machines," in *IEEE Transactions on Magnetics*, vol. 52, no. 3, pp. 1-4, March 2016
- [11] Y. Wang, D. M. Ionel, V. Rallabandi, M. Jiang and S. J. Stretz, "Large-Scale Optimization of Synchronous Reluctance Machines Using CE-FEA and Differential Evolution," in *IEEE Transactions on Industry Applications*, vol. 52, no. 6, pp. 4699-4709, Nov.-Dec. 2016
- [12] H. Cai, B. Guan and L. Xu, "Low-Cost Ferrite PM-Assisted Synchronous Reluctance Machine for Electric Vehicles," in *IEEE Transactions on Industrial Electronics*, vol. 61, no. 10, pp. 5741-5748, Oct. 2014
- [13] Y. Wang, D. M. Ionel, M. Jiang and S. J. Stretz, "Establishing the Relative Merits of Synchronous Reluctance and PM-Assisted Technology Through Systematic Design Optimization," in *IEEE Transactions on Industry Applications*, vol. 52, no. 4, pp. 2971-2978, July-Aug. 2016
- [14] C. M. Spargo, B. C. Mecrow and J. D. Widmer, "A Seminumerical Finite-Element Postprocessing Torque Ripple Analysis Technique for Synchronous Electric Machines Utilizing the Air-Gap Maxwell Stress Tensor," in *IEEE Transactions on Magnetics*, vol. 50, no. 5, pp. 1-9, May 2014
- [15] Ion Boldea, *Reluctance Synchronous Machines and Drives* (Monographs in Electrical and Electronic Engineering), OUP Oxford, 2002
- [16] D. A. Staton, T. J. E. Miller and S. E. Wood, "Maximising the saliency ratio of the synchronous reluctance motor," in *IEE Proceedings B - Electric Power Applications*, vol. 140, no. 4, pp. 249-259, July 1993
- [17] Pyrhonen, J., T. Jokinen, and V. Hrabovcová. "Design of Rotating Machines." (2008)
- [18] C. Donaghy-Spargo; B. C. Mecrow; J. D. Widmer, "Electromagnetic Analysis of a Synchronous Reluctance Motor with Single Tooth Windings," in *IEEE Transactions on Magnetics*, vol. 99, pp. 1-1
- [19] A. M. EL-Refaie, "Fractional-Slot Concentrated-Windings Synchronous Permanent Magnet Machines: Opportunities and Challenges," in *IEEE Transactions on Industrial Electronics*, vol. 57, no. 1, pp. 107-121, Jan. 2010
- [20] J. Gieras, "Permanent Magnet Motor Technology", CRC Press, 2010
- [21] P. Ponomarev, Y. Alexandrova, I. Petrov, P. Lindh, E. Lomonova and J. Pyrhönen, "Inductance Calculation of Tooth-Coil Permanent-Magnet Synchronous Machines," in *IEEE Transactions on Industrial Electronics*, vol. 61, no. 11, pp. 5966-5973, Nov. 2014
- [22] P. Ponomarev, P. Lindh and J. Pyrhönen, "Effect of Slot-and-Pole Combination on the Leakage Inductance and the Performance of Tooth-Coil Permanent-Magnet Synchronous Machines," in *IEEE Transactions on Industrial Electronics*, vol. 60, no. 10, pp. 4310-4317, Oct. 2013
- [23] IEEE Std 115-2009 - IEEE Guide for Test Procedures for Synchronous Machines Part I - Acceptance and Performance Testing; Part II - Test Procedures and Parameter Determination for Dynamic Analysis
- [24] R. Betz, Chapter 8: Modelling and Control of Synchronous Reluctance Motors, in "Control in Power Electronics: Selected Problems", Academic Press, 2002

APPENDIX

Four pole ($p = 2$) synchronous reluctance machines are almost universally found in the literature. Simple reasons for this are the reduction in stator core sizing compared to a two pole ($p = 1$) variant and the relative ease in which the flux barriers can be shaped. The stator leakage inductance $L_{s\sigma}$ also has an impact on the power factor as the number of poles p increases. The main inductance of a three-phase machine can be expressed as follows;

$$L_m = \frac{3D_\delta L\mu_0}{\pi p^2 \delta_{\text{eff}}} (Nk_{w1})^2 \propto f\left(\frac{1}{p^2}\right) \quad (\text{A1})$$

Where D_δ is the air-gap diameter, δ_{eff} is the effective airgap and Nk_{w1} the effective number of series turns per phase. Thus, the main magnetizing inductance has an inverse square law dependence on the number of rotor poles. However, the expression for the stator leakage inductance, Eq. (10), is not a function of p , therefore, for a set of stator dimensions, the per unit leakage inductance increases, lowering the power factor, as the number of poles increases.



C. M. Donaghy-Spargo received the BEng (Hons) and PhD degrees in Electrical Engineering from Newcastle University, Newcastle upon Tyne, U.K. He was a Motor Drives Engineer (Research) at Dyson, UK, before entering his current position as Assistant Professor of Electrical Engineering in the Department of Engineering, Durham University, UK. His research interests include the design, modelling and control of high efficiency and high performance electrical machines, with a specific interest in synchronous reluctance machines. He is actively involved with the Institution of Engineering and Technology, UK..



B. C. Mecrow received the Ph.D. degree from the University of Newcastle upon Tyne, Newcastle upon Tyne, U.K., for his research into 3-D eddy-current computation applied to turbogenerators. He commenced his career as a Turbogenerator Design Engineer with NEI Parsons, Newcastle upon Tyne, U.K. He became a Lecturer in 1987 and a Professor in 1998 with Newcastle University, Newcastle upon Tyne. He is the Head of the School of Electrical and Electronic Engineering, Newcastle University, where he is also a Professor of electrical power engineering. His research interests include fault-tolerant drives, high-performance permanent-magnet machines, and novel switched reluctance drives.



J. D. Widmer is responsible for Newcastle University's 'Centre for Advanced Electrical Drives'. Part of the University's Power Electronics, Drives and Machines Research group, the Centre works with numerous Industry partners to convert academic research into world class products. James' research interests include rare-earth magnet free motor topologies for the automotive industry, including Switched Reluctance and other Motor types, as well as including research into high performance and high

efficiency Permanent Magnet machines. James joined Newcastle University in 2009 from a senior post in the Aerospace Industry.